

EFFECTS OF THERMODYNAMIC PAIRING ON NUCLEAR LEVEL DENSITY

NGUYEN QUANG HUNG

Tan Tao University

DANG THI DUNG AND TRAN DINH TRONG

Institute of Physics, VAST

Abstract. *Thermodynamic properties of some selected even-even nuclei such as ^{56}Fe , ^{60}Ni , ^{98}Mo , and ^{116}Sn are studied within the Bardeen-Cooper-Schrieffer theory at finite temperature (FTBCS) taking into account pairing correlations. The theory also incorporates the particle-number projection within the Lipkin-Nogami method (FTLN). The level densities are derived based on the statistical theory of the grand-canonical ensemble (GCE). The results obtained are compared with the recent experimental data by Oslo (Norway) group. It is found that pairing correlations have significant effects on nuclear level density, especially at low and intermediate excitation energies.*

I. INTRODUCTION

Pairing is a common feature in strongly interacting many-body systems ranging from very large ones such as superconductors or neutron stars to very small ones as atomic nuclei or superconducting ultra-small metallic grains [1]. Pairing correlations have significant effects on the physical properties of atomic nuclei such as the binding and excitation energies, collective motions, rotations, level densities, etc. The Bardeen-Cooper-Schrieffer (BCS) theory [2], a theory of superconductivity, has been widely employed to describe the pairing properties of not only infinite but also finite systems such as atomic nuclei (see e.g. Refs. [3, 4]). At finite temperature T , the finite-temperature BCS (FTBCS) theory predicts a pairing gap which decreases with increasing T and collapses at a given critical temperature $T_C \approx 0.568\Delta(0)$ with $\Delta(0)$ being the pairing gap at zero temperature [4]. As the result, the system undergoes a sharp phase transition from superfluid to normal ones (SN phase transition). This prediction is in very good agreement with the experimental measurements in infinite systems such as metallic superconductors. However, the FTBCS theory fails to describe the pairing properties of finite small systems such as atomic nuclei. One of the reason is due to the fact that the FTBCS theory violates the particle-number conservation, which is negligible in infinite systems but significant in the finite ones. One simple method to resolve the particle-number problem of the FTBCS theory is to apply the particle-number projection (PNP) proposed by Lipkin-Nogami (LN) [5]. The LN method is an approximate PNP before variation, which has been widely used in nuclear physics. In this work, we apply the FTBCS theory as well as the FTBCS with Lipkin-Nogami PNP to describe the thermodynamic properties and level densities of some selected even-even nuclei (the numbers of neutrons N and protons Z are even) such as ^{56}Fe , ^{60}Ni ,

^{98}Mo , and ^{116}Sn . The results obtained are then compared with the corresponding data, which have recently measured by Oslo (Norway) group [6, 7].

II. FORMALISM

The present paper considers a pairing Hamiltonian [8]

$$H = \sum_k \epsilon_k (a_k^\dagger a_k + a_{-k}^\dagger a_{-k}) - G \sum_{kk'} a_k^\dagger a_{-k}^\dagger a_{-k'} a_{k'} \quad (1)$$

which describes a system of N particles with single-particle energy ϵ_k interacting via a constant monopole force G . Here a_k^\dagger and a_k denote the particle creation and annihilation operators. The subscripts k are used to label the single-particle states $|k, m_k\rangle$ in the deformed basis with the positive single-particle spin projections m_k , whereas the subscripts $-k$ denote the time-reversal states $|k, -m_k\rangle$.

II.1. FTBCS equations

The FTBCS equations are derived based on the variational procedure to minimize the Hamiltonian $H_{\text{BCS}} = H - \lambda \hat{N}$, where

$$\hat{N} = \sum_k \left(a_k^\dagger a_k + a_{-k}^\dagger a_{-k} \right), \quad (2)$$

is the particle-number operator and λ is the chemical potential. At finite temperature, the minimization procedure is done within the grand canonical ensemble (GCE) average, in which the expectation value of any operator \hat{O} is given as [9]

$$\langle \hat{O} \rangle = \frac{\text{Tr}[\hat{O} e^{-\beta H}]}{\text{Tr} e^{-\beta H}}, \quad (3)$$

with $\beta = 1/T$ being the invert of temperature. The FTBCS equations for the pairing gap Δ and particle number N have the form as:

$$\begin{aligned} \Delta &= G \sum_k \tau_k; & N &= 2 \sum_k \rho_k, \\ \tau_k &= u_k v_k (1 - 2n_k); & \rho_k &= (1 - 2n_k) v_k^2 + n_k, \\ u_k^2 &= \frac{1}{2} \left(1 + \frac{\epsilon_k - \lambda - G v_k^2}{E_k} \right); & v_k^2 &= 1 - u_k^2, \\ E_k &= \sqrt{(\epsilon_k - \lambda - G v_k^2)^2 + \Delta^2}, \end{aligned} \quad (4)$$

where the quasiparticle occupation number n_k is given in terms of the Fermi-Dirac distribution of free quasiparticle

$$n_k = \frac{1}{1 + e^{\beta E_k}}. \quad (5)$$

The total (internal) energy E_{FTBCS} , heat capacity C_{FTBCS} , and entropy S_{FTBCS} obtained within the FTBCS are given as

$$\begin{aligned} E_{\text{FTBCS}}(T) &= 2 \sum_k \epsilon_k \rho_k - \frac{\Delta^2}{G} - G \sum_k v_k^4 (1 - 2n_k), \\ C_{\text{FTBCS}}(T) &= \frac{\partial E_{\text{FTBCS}}}{\partial T}, \\ S_{\text{FTBCS}}(T) &= -2 \sum_k [n_k \ln n_k + (1 - n_k) \ln(1 - n_k)]. \end{aligned} \quad (6)$$

II.2. FTBCS equations with Lipkin-Nogami particle-number projection (FTLN equations)

It is well-known that the BCS theory violates the particle number because the BCS wave function is not an eigenstate of the particle-number operator \hat{N} . To resolve this problem of the BCS, we employ here an approximate particle-number projection within the Lipkin-Nogami method [5]. The FTLN equations are obtained by carrying out the variational calculations (within the GCE) to minimize the Hamiltonian

$$H_{LN} = H - \lambda_1 \hat{N} - \lambda_2 \hat{N}^2. \quad (7)$$

As the result, the FTLN equations for the pairing gap and particle number have the form as [10]

$$\begin{aligned} \Delta &= G \sum_k \tau_k; \quad N = 2 \sum_k \rho_k, \\ \tau_k &= u_k v_k (1 - 2n_k); \quad \rho_k = (1 - 2n_k) v_k^2 + n_k, \\ u_k^2 &= \frac{1}{2} \left(1 + \frac{\epsilon'_k - \lambda - G v_k^2}{E_k} \right); \quad v_k^2 = 1 - u_k^2, \\ E_k &= \sqrt{(\epsilon'_k - \lambda - G v_k^2)^2 + \Delta^2}; \quad n_k = \frac{1}{1 + e^{\beta E_k}} \\ \epsilon'_k &= \epsilon_k + (4\lambda_2 - G) v_k^2; \quad \lambda = \lambda_1 + 2\lambda_2 (N + 1), \\ \lambda_2 &= \frac{G \sum_k (1 - \rho_k) \tau_k \sum_{k'} \rho_{k'} \tau_{k'} - \sum_k (1 - \rho_k^2) \rho_k^2}{4 [\sum_k (1 - \rho_k) \rho_k]^2 - \sum_k (1 - \rho_k^2) \rho_k^2}. \end{aligned} \quad (8)$$

The FTLN total energy, heat capacity, and entropy are then given as

$$\begin{aligned} E_{\text{FTLN}}(T) &= 2 \sum_k \epsilon_k \rho_k - \frac{\Delta^2}{G} - G \sum_k v_k^4 (1 - 2n_k) - \lambda_2 \Delta N^2, \\ C_{\text{FTLN}}(T) &= \frac{\partial E_{\text{FTLN}}}{\partial T}, \\ S_{\text{FTLN}}(T) &= -2 \sum_k [n_k \ln n_k + (1 - n_k) \ln(1 - n_k)], \end{aligned} \quad (9)$$

where $\Delta N^2 = \left| \langle \hat{N} \rangle^2 - \langle \hat{N}^2 \rangle \right|$ is the particle-number fluctuation, whose explicit forms can be found for example in Ref. [12], namely

$$\Delta N^2 = \Delta N_{QF}^2 + \Delta N_{SF}^2, \quad (10)$$

where ΔN_{QF}^2 are the quantal fluctuations (QF), whereas ΔN_{SF}^2 are the statistical fluctuations (SF) of the particle number

$$\begin{aligned} \Delta N_{QF}^2 &= 4 \sum_k u_k^2 v_k^2 (1 - 2n_k), \\ \Delta N_{SF}^2 &= 2 \sum_k 2(u_k^2 - v_k^2)^2 n_k (1 - n_k) + 8 \sum_k u_k^2 v_k^2 n_k. \end{aligned} \quad (11)$$

II.3. Level density

Level density is derived based on the statistical theory of the grand-canonical ensemble (GCE). Within the GCE, the density of state is calculated as [11]

$$\omega(E^*) = \frac{e^S}{(2\pi)^{3/2} D^{1/2}}, \quad (12)$$

where S is the total (neutron + proton) entropy, obtained within the FTBCS [Eq. (6)] or FTLN [Eq. (9)], and

$$D = \begin{vmatrix} \frac{\partial^2 \Omega}{\partial \alpha_N^2} & \frac{\partial^2 \Omega}{\partial \alpha_N \partial \alpha_Z} & \frac{\partial^2 \Omega}{\partial \alpha_N \partial \beta} \\ \frac{\partial^2 \Omega}{\partial \alpha_Z \partial \alpha_N} & \frac{\partial^2 \Omega}{\partial \alpha_Z^2} & \frac{\partial^2 \Omega}{\partial \alpha_Z \partial \beta} \\ \frac{\partial^2 \Omega}{\partial \beta \partial \alpha_N} & \frac{\partial^2 \Omega}{\partial \beta \partial \alpha_Z} & \frac{\partial^2 \Omega}{\partial \beta^2} \end{vmatrix}, \quad (13)$$

with $\alpha = \beta\lambda$, and Ω being the logarithm of the grand partition function

$$\Omega = \ln \left[\text{tr}(e^{-\beta H}) \right] = -\beta \sum_k (\epsilon_k - \lambda - E_k) + 2 \sum_k \ln(1 + e^{-\beta E_k}) - \beta \frac{\Delta^2}{G}. \quad (14)$$

Finally, the level density is defined as

$$\rho(E^*) = \frac{\omega(E^*)}{\sigma \sqrt{2\pi}}, \quad (15)$$

where

$$\sigma^2 = \frac{1}{2} \sum_k m_k^2 \text{sech}^2 \frac{1}{2} \beta E_k, \quad (16)$$

is the spin cut-off parameter. In Eqs. (12) and (15), the excitation energy E^* is calculated from the total energy as

$$E^*(T) = E(T) - E_{g.s}(T=0), \quad (17)$$

where $E_{g.s}$ is the ground-state (binding) energy, which is the sum of the FTBCS or FTLN energy at $T=0$ plus the corrections due to the Wigner E_{Wigner} and deformation energies E_{def}

$$E_{g.s}(T=0) = E_{g.s}^{\text{FTBCS(FTLN)}}(T=0) + E_{Wigner} + E_{def}. \quad (18)$$

Table 1. The values of pairing interaction parameter G_N and G_Z and the corresponding pairing gaps Δ_N and Δ_Z obtained within the FTLN.

	⁵⁶ Fe	⁶⁰ Ni	⁹⁸ Mo	¹¹⁶ Sn
G_N (MeV)	0.312	0.340	0.193	0.170
Δ_N (MeV)	1.400	1.840	1.200	1.140
G_Z (MeV)	0.437	0.000	0.314	0.000
Δ_Z (MeV)	1.600	0.000	1.210	0.000

Here, for simplicity E_{Wigner} and E_{def} are estimated from the Hartree-Fock-Bogoliubov (HFB) calculations with Skyrme BSk14 interaction [12].

III. NUMERICAL RESULTS AND DISCUSSIONS

III.1. Ingredients of numerical calculations

The numerical calculations are carried out for some selected even-even nuclei, namely ⁵⁶Fe, ⁶⁰Ni, ⁹⁸Mo, and ¹¹⁶Sn. The single-particle energies are obtained within the axial deformed Woods-Saxon (WS) potential including the spin-orbit and Coulomb interactions [13]. The depth of the WS central potential is given as

$$V = V_0 \left[1 \pm k \frac{N - Z}{N + Z} \right], \quad (19)$$

where $V_0 = 51.0$ MeV, $k = 0.86$, and the plus and minus signs stand for proton (Z) and neutron (N), respectively. The radius r_0 , diffuseness a , and spin-orbit strength λ are chosen to be $r_0 = 1.27$ fm, $a = 0.67$ fm, and $\lambda = 35.0$. The quadrupole deformation parameters β_2 for ⁵⁶Fe and ⁹⁸Mo are chosen to be the same as that of Ref. [14], namely $\beta_2 = 0.24$ for ⁵⁶Fe and $\beta_2 = 0.17$ for ⁹⁸Mo, whereas those for two spherical nuclei ⁶⁰Ni and ¹¹⁶Sn are equal to zero. All the single-particle levels with negative energies (bound states) are taken into account. The pairing interaction parameters G are adjusted so that the pairing gaps for neutron and proton obtained within the FTLN at $T = 0$ reproduce the corresponding values extracted from the experimental odd-even mass differences [15]. The values of G_N , G_Z , Δ_N , and Δ_Z are given in Table 1. It is worth mentioning that the FTBCS and FTLN are derived from the pairing Hamiltonian (1), in which the pairing interaction parameter G was there already from the beginning of the derivation processes. It means that G does not change or is not renormalized within the FTBCS and FTLN. Obviously, there is no physical justification of choosing different G for different approaches (FTBCS and FTLN), which derive from the same Hamiltonian. Indeed, G should be chosen to be the same for both FTBCS and FTLN (See e.g. Refs. [10, 16]). Moreover, since the FTBCS violates the particle-number conservation as discussed in Sec. II.2, the FTLN resolves the particle-number problem of the FTBCS by projecting the components of the BCS wave function onto good particle number states, which makes the FTLN prediction for the pairing gap become more precisely than the FTBCS one. Therefore, it is reasonable and consistent for the adjustment of G to obtain the FTLN gap at $T=0$ being the same as the empirical gap obtained from the experimental odd-even mass difference.

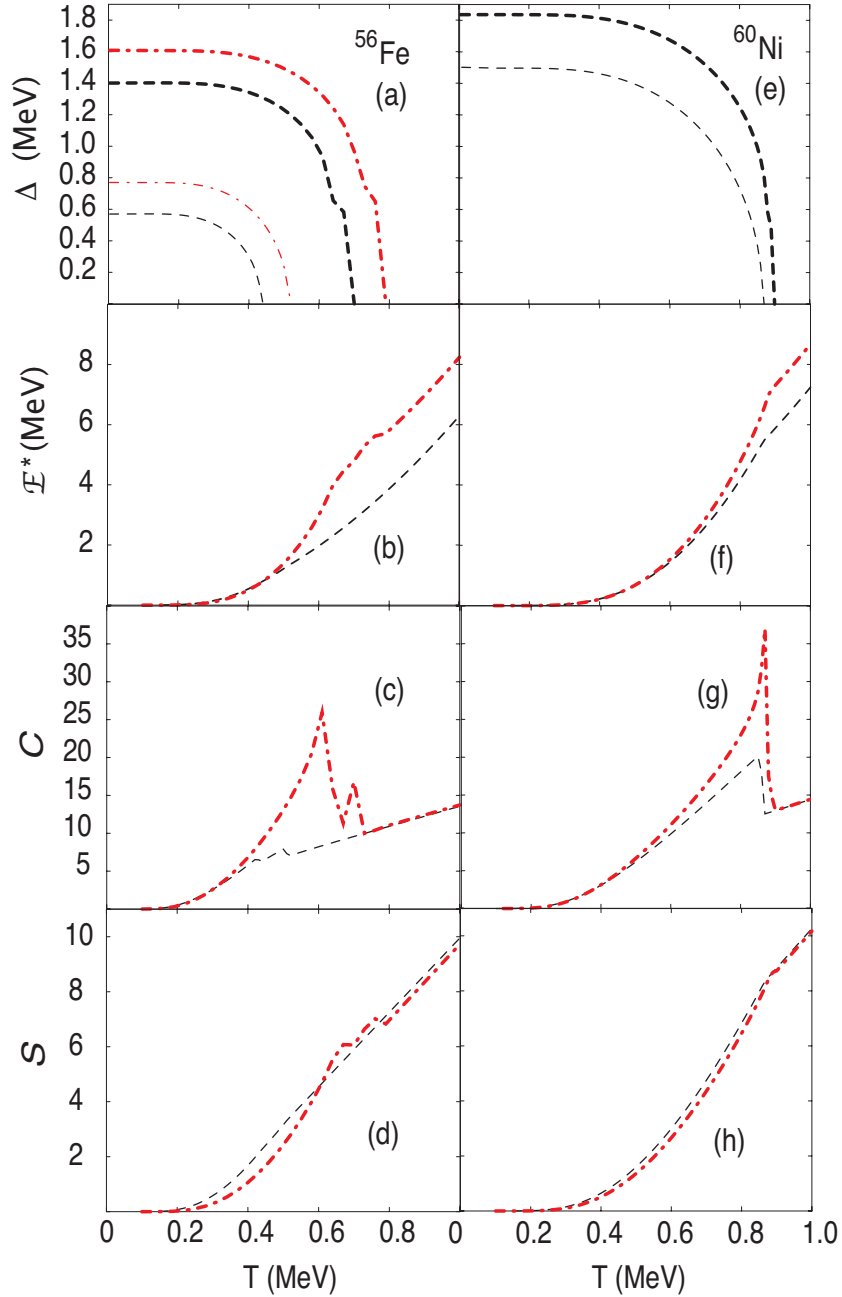


Fig. 1. (Color online) Pairing gaps Δ (neutron and proton), total (neutron + proton) excitation energy E^* , total heat capacity C , and total entropy S as functions of temperature T for ^{56}Fe (left panels) and ^{60}Ni (right panels). In Figs 1. (a) and (e), the thin and thick dashed lines denote the neutron pairing gaps Δ_N , whereas the thin and thick dash dotted lines stand for the proton pairing gaps Δ_Z . Here the thin lines show the results obtained within the FTBCS, whereas the thick lines present the FTLN results. In Figs. 1 [(b) (d)] and [(f) (h)], the thin dashed and thick dash dotted lines depict the FTBCS and FTLN total results for neutrons plus protons, respectively.

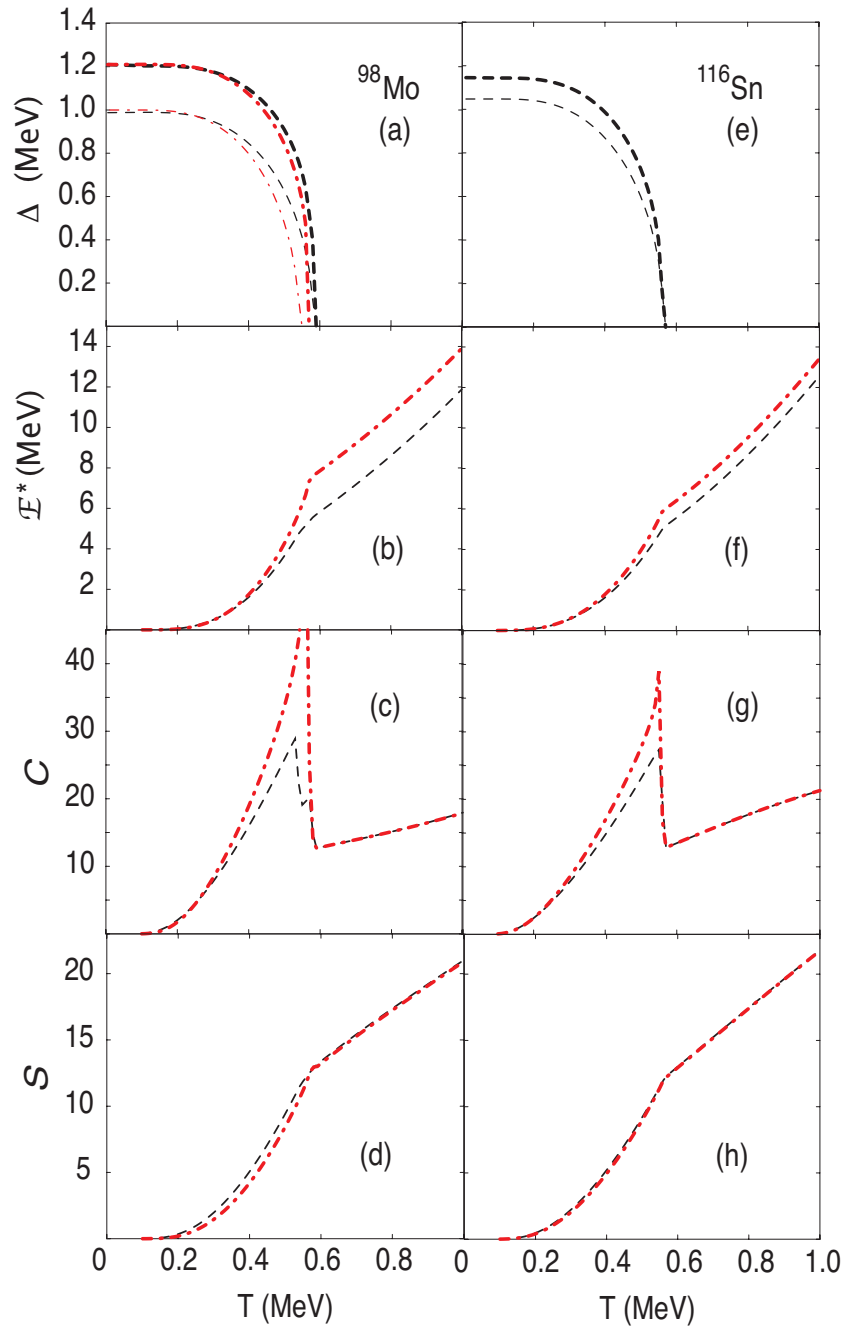


Fig. 2. (Color online) Same as Fig. 1 but for ^{98}Mo and ^{116}Sn .

Table 2. The values of critical temperature T_C obtained within the FTBCS and FTLN calculations for neutrons and protons in ^{56}Fe , ^{60}Ni , ^{98}Mo , and ^{116}Sn isotopes.

	$T_C^{\text{FTBCS}}(\text{MeV})$		$T_C^{\text{FTLN}}(\text{MeV})$	
	Neutron	Proton	Neutron	Proton
^{56}Fe	0.44	0.52	0.7	0.79
^{60}Ni	0.87	0.00	0.90	0.00
^{98}Mo	0.59	0.55	0.59	0.57
^{116}Sn	0.57	0.00	0.57	0.00

III.2. Thermodynamic quantities

The thermodynamic quantities such as pairing gaps Δ , excitation energies E^* , heat capacities C , and entropies S obtained within the FTBCS (dashed lines) and FTLN (dash dotted line) for ^{56}Fe , ^{60}Ni , ^{98}Mo , and ^{116}Sn are plotted in Figs. 1 and 2. It is clear to see from these Figs. 1 and 2 that the FTBCS gaps (thin lines) decrease with increasing T and vanish at a given critical temperature $T = T_C$ resulting the sharp peaks located near T_C in the heat capacity C , which is the signature of SN phase transition. By applying the particle-number projection within the Lipkin-Nogami method, the FTLN pairing gaps at $T = 0$ (thick lines) are always higher than that of the FTBCS. As the result, the FTLN gap collapses at a critical temperature T_C , which is higher than the corresponding FTBCS value. The values of T_C obtained within the FTBCS and FTLN for all nuclei are given in Table 2. It is worth mentioning that T_C for neutron and proton are different resulting two peaks in the results of heat capacity C [See e.g. Figs. 1 (c) and (g) or 2 (c) and (g)]. The difference between the thermodynamic quantities obtained within the FTBCS and FTLN in light nuclei like ^{56}Fe is stronger than in heavy nuclei like ^{116}Sn as seen in Figs. 1 and 2. This is well-known due to the fact that the particle-number fluctuation in the light systems is usually stronger than in the heavy ones. It is noticing that the proton gaps of ^{60}Ni and ^{116}Sn are zero because these two nuclei have proton magic numbers ($Z = 28$ for ^{60}Ni and $Z = 50$ for ^{116}Sn). Consequently, Figs. 1 [(a), (e)] and 2 [(a), (e)] show the neutron gaps only, whereas the corresponding T_C values are zero as shown in Table 2.

III.3. Level density

Shown in Fig. 3 are the level densities obtained within the FTBCS and FTLN as well as the case without pairing ($\Delta = 0$) versus the experimental data taken from Refs. [6, 7]. This Fig. 3 shows very clearly that the level densities obtained within the FTLN fit best the experimental data for all nuclei. Since the FTBCS gaps are always lower than the FTLN ones, the level densities obtained within the FTBCS overestimate the experimental data, whereas those obtained within the $\Delta = 0$ case are quite far from the experimental ones. The jumps seen in the level densities obtained within the FTBCS and FTLN correspond to the collapsing of the pairing gaps at T_C as mentioned above. The ground-state energy corrections by Wigner and deformation energies, which shift up the total excitation energy E^* toward the right direction to the experimental data, are also important in present case. Consequently, we can conclude that the pairing correlations

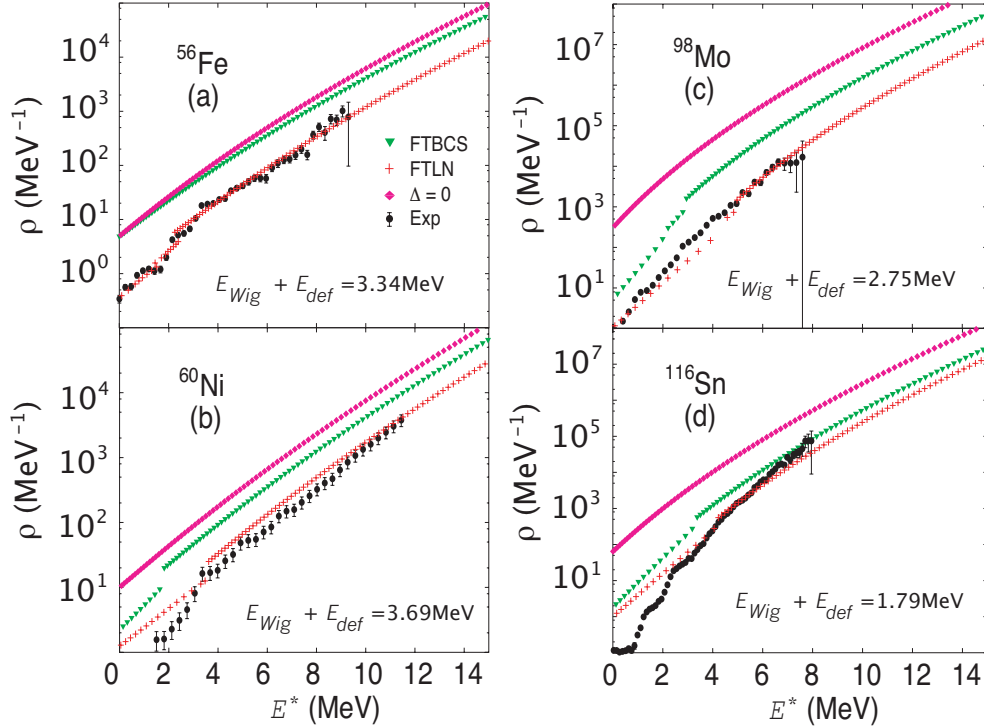


Fig. 3. (Color online) Level density ρ as function of total excitation energy E^* obtained within the FTBCS (triangles), FTLN (crosses) and the case without pairing ($\Delta = 0$) (rectangles) versus the experimental data (full circles with error bars) for ^{56}Fe (a), ^{60}Ni (b), ^{98}Mo (c) and ^{116}Sn (d). The values of ground-state (binding) energy corrections $E_{Wigner} + E_{def}$ are shown in the figures..

together with the particle-number conservation within the Lipkin-Nogami method as well as the corrections for the ground-state energy due to the Wigner isospin symmetry and deformation are all important for the description of nuclear level density.

III.4. Justification of choosing pairing interaction parameter G

Although there is no physical justification that one could choose different G for different approaches as discussed in Sec. III.1, we make here a test by adjusting G so that the gaps obtained within both FTBCS and FTLN at $T = 0$ fit to the experimental values. The results for the pairing gap are shown in Fig. 4, whereas those for the level densities are plotted in Fig. 5. The results in Fig. 4 shows that by choosing different G the gaps obtained within the FTBCS and FTLN are almost the same at low T region (around $0 \leq T \leq 0.5$ MeV). At $T > 0.5$ MeV, the FTBCS gap decreases slower than the FTLN one leading the T_C obtained within the FTBCS being higher than that obtained within the FTLN. As a result, by comparing the results shown in Fig. 3 with those plotted in Fig. 5, the level densities obtained within the FTBCS become closer to the FTLN results but they are still higher than the FTLN as well as the experimental values. Once again, the

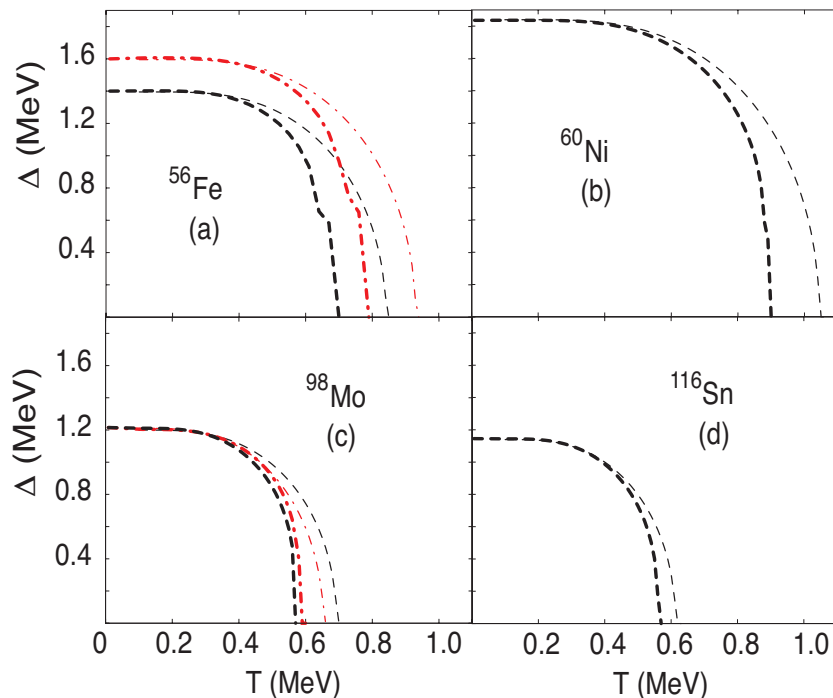


Fig. 4. (Color online) Pairing gaps Δ (neutron and proton) obtained within the FTBCS and FTLN by adjusting G to fit their gaps obtained at $T = 0$ to the experimental values. Notations are the same as in Fig. 1.

results of this test confirm that the FTLN offers a better or more precisely thermodynamic pairing as well as level density than the FTBCS one.

IV. CONCLUSION

Present paper applies the finite-temperature BCS (FTBCS) theory as well as the FTBCS with the approximate particle-number projection within the Lipkin-Nogami method (FTLN) to describe the thermodynamic properties as well as level densities of several selected even-even isotopes, namely ^{56}Fe , ^{60}Ni , ^{98}Mo , and ^{116}Sn . The corrections for the ground-state (binding) energy by means of the Wigner and deformation energies are also taken into account. The level densities obtained within the FTLN fit best experimental data, whereas those obtained within the FTBCS deviate from the experimental one. The reason is that the FTLN theory predicts more reasonable pairing gaps as well as other thermodynamic quantities than the FTBCS one. As the result, we conclude that the pairing correlations, the corrections due to the particle-number fluctuation and the corrections for the binding energy all together have significant effects on the nuclear level density, especially at low and intermediate excitation energies. In present work, the effects of thermal fluctuations, which have recently found to be very important in small systems such as atomic nuclei [17], are still neglected. As the next step, we will study the effects

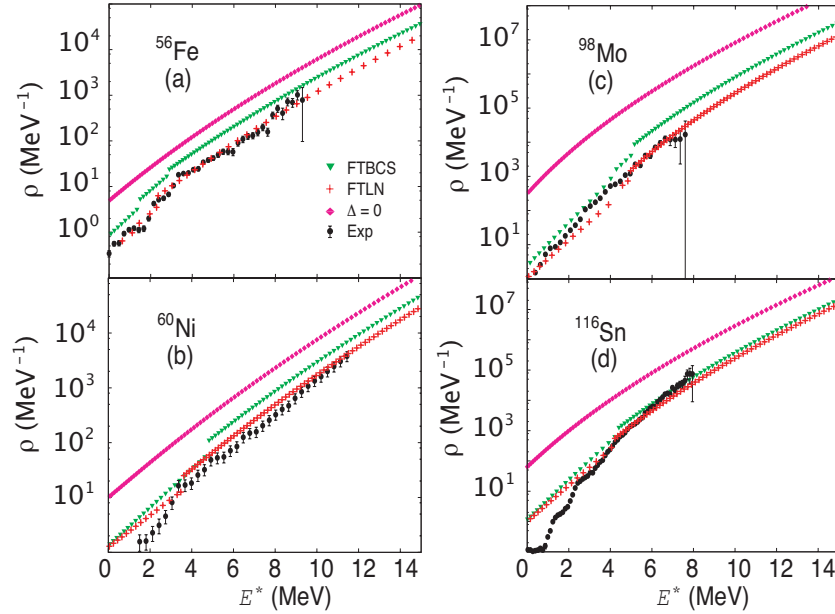


Fig. 5. (Color online) Same as Fig. 3 but for the case which uses different G for the FTBCS and FTLN as discussed in Sec. III.4.

of thermal fluctuations on the nuclear level density by using the theoretical approaches developed in Refs. [8, 10]. This work is now underway.

ACKNOWLEDGMENT

The authors acknowledge the support by the National Foundation for Science and Technology Development (NAFOSTED) through Grant No. 103.04-2010.02. We also thank Dr. Tran Viet Nhan Hao (Tan Tao University) for his critical readings, comments and suggestions to present manuscript.

REFERENCES

- [1] D. J. Dean and M. Hjorth-Jensen, *Rev. Mod. Phys.* **75** (2003) 607.
- [2] J. Bardeen, L. Cooper, and J. Schrieffer, *Phys. Rev.* **108** (1957) 1175.
- [3] L. G. Moretto, *Phys. Lett.* **B 40** (1972) 1.
- [4] A. L. Goodman, *Nucl. Phys.* **A 352** (1981) 30; *Phys. Rev.* **C 29** (1984) 1887.
- [5] H. J. Lipkin, *Ann. Phys.* (NY) **9** (1960) 272; Y. Nogami and I. J. Zucker, *Nucl. Phys.* **60** (1964) 203; Y. Nogami, *Phys. Lett.* **15** (1965) 4.
- [6] E. Melby *et al.*, *Phys. Rev. Lett.* **83** (1999) 3150; A. Schiller *et al.*, *Phys. Rev.* **C63** (2001) 021306(R); E. Algin *et al.*, *Phys. Rev.* **C 78** (2008) 054321.
- [7] M. Guttormsen *et al.*, *Phys. Rev.* **C62** (2000) 024306; R. Chankova *et al.*, *Phys. Rev.* **C73** (2006) 034311.
- [8] N. Quang Hung and N. Dinh Dang, *Phys. Rev.* **C78** (2008) 064315.
- [9] N. Dinh Dang, *Nucl. Phys.* **A 784** (2007) 147.
- [10] N. Dinh Dang and N. Quang Hung, *Phys. Rev.* **C77** (2008) 064315

- [11] L. G. Moretto, *Nucl. Phys.* **A185** (1972) 145; A. N. Behkami and J. R. Huizenga, *Nucl. Phys.* **A 217** (1973) 78.
- [12] S. Hilaire and S. Goriely, *Nucl. Phys.* **A779** (2006) 63; S. Goriely, S. Hilaire, and A. J. Koning, *Phys. Rev.* **C78** (2008) 064307.
- [13] S. Cwiok *et al.*, *Comput. Phys. Commun.* **46** (1987) 379.
- [14] S. Liu and Y. Alhassid, *Phys. Rev. Lett.* **87** (2001) 022501; K. Kaneko *et al.*, *Phys. Rev.* **C74** (2006) 024325.
- [15] P. Ring and P. Schuck, *The Nuclear Many-Body Problem* (Springer-Verlag, New York, 1980).
- [16] N. Quang Hung and N. Dinh Dang, *Phys. Rev.* **C79** (2009) 054328; *ibid.* **81** (2010) 057302; **82** (2010) 044316.
- [17] V. Zelevinsky, B. A. Brown, N. Frazier, and M. Horoi, *Phys. Rep.* **276** (1996) 85; N. Dinh Dang and V. Zelevinsky, *Phys. Rev.* **C64** (2001) 064319; N. Dinh Dang and A. Arima, *Phys. Rev.* **C67** (2003) 014304.

Received 15 February 2012.